MRS Advances © 2018 Materials Research Society DOI: 10.1557/adv.2018.128

Synthesis, microstructure, and mechanical properties of polycrystalline Cu nano-foam

Chang-Eun Kim¹, Raheleh M. Rahimi¹, Nia Hightower¹, Ioannis Mastorakos², and David F. Bahr^{1,*}

Abstract

A polycrystalline Cu foam with sub-micron ligament sizes was formed by creating a nonwoven fabric via electrospinning with a homogeneous mixture of polyvinyl alcohol(PVA)-and copper acetate(Cu(Ac)₂). Thermogravimetric measurement of the electrospun fabric of the precursor solution is reported. Oxidizing the precursor fabric at 773K formed an oxide nanofoam; subsequent heating at 573K with a reducing gas transformed the CuO nano-foam to Cu with a similar ligament and meso-scale pore size morphology. A cross-section prepared by focused ion beam lift-out shows the polycrystalline structure with multi-scale porosity. The mechanical property of the Cu nano-foam is measured by nano-indentation. The load-depth curves and deduced mechanical properties suggest that additional intra-ligament pores lead to unique structure-property relations in this non-conventional form of metal.

INTRODUCTION

Metallic nano-foams are attractive materials for catalysis due to their extremely low density and high specific surface area. Dealloying precious metals has been widely used to study porous metal phases,[1] however, this method has several limitations. Dealloying limits exist in the choice of metal phase, the accessible density domain, and the microstructure of the resulting ligaments. The fact that the crystal structure of the host metal prior to deposition remains in the porous structure means the vast majority of dealloyed films consist of single crystal ligaments.[2] Two physical aspects that made the dealloying method particularly useful in studying low-density metal foams are: (i) spatially confined diffusion and coalescence of the alloy components, and (ii) removal of the unnecessary frame material, e.g. by using chemical etchant in the case of conventional dealloying process.

In the present work, we report a synthesis of low-density nanoscale metallic foams that can facilitate further exploration of the strength-density relation of porous materials. Using an electrospun non-woven polymer fabric as a sacrificial template enables the confined diffusion and coalescence of the metal nuclei. In this templated synthesis route, the choice of constituent metal species is determined by the solubility of precursor in the electrospinning process instead of an element's reduction potential, as in

School of Materials Engineering, Purdue University, 701 W. Stadium Ave, West Lafayette, IN 47906-

² Department of Mechanical and Aeronautical Engineering, Clarkson University, Potsdam, NY 13699, USA

https://doi.org/10.1557/adv.2018.128

the dealloying method. Electrospinning provides scalability to the synthesis of nanoscale metal foams.[3] Removal of the polymer template is achieved by pyrolysis instead of using chemical etchants. In the present approach, the metal precursors decompose and nucleate inside the polymer template. Further coalescence proceeds as the polymer network undergoes thermal decomposition and shrinkage, in short, the nucleation-diffusion mechanism dictates the microstructure of the nano-foam in the present approach. In comparison the microstructure from the dealloying method is not dictated by nucleation mechanism. As a result the templated synthesis method creates a fundamentally different microstructure distinct from that of dealloying method.

METHODOLOGY

The electrospinning of PVA-Cu(Ac)₂ fiber was carried out by using a Spellman SL300 high voltage controller. The external voltage was set to 15kV, the target was placed 12 cm away from the syringe tip, and the current limit was set as 2 mA. The deposition was carried out for 30 minutes. The PVA-Cu(Ac)₂ electrospinning solution was prepared by mixing deionized water, polyvinyl alcohol (MW=124k-186k, Aldrich, 87-89% hydrolyzed), and copper(II) acetate monohydrate (Fisher Scientific Acros, ACS Reagent grade) in 8.4:0.6:0.84 by mass ratio at room temperature. The syringe pump speed was 0.17mL/h. Commercially available aluminum foil (24 µm thickness) was placed on a target holder made of 3D-printed poly-lactic acid to collect the fibers. Once collected on Al foil, the sample was dried in ambient atmosphere for 30 minutes, mechanically detached from the foil, and then processed with subsequent thermal treatments.

The first heat treatment was carried out to burn-off the PVA. The temperature was increased from room temperature to 500 °C at 5 °C/min, held for 2 hours, and then cooled to room temperature at approximately 5 °C/min. The electrospun PVA/Cu(Ac)₂ fibers undergo thermal decomposition, leaving a CuO nano-foam behind. A substantial macroscopic shrinkage of the electrospun fabric was observed, likely why a distinct foam structure was obtained instead of a fused wire network observed in previous studies.[4] The thermal decomposition profile was obtained by thermogravimetric scanning from 25 °C to 500 °C by a ramping rate of 5 °C/min, using TGA-Q50 (TA instruments Inc.).

The CuO nano-foam specimens were thermally processed in a reducing gas atmosphere (95% Ar, 5% $\rm H_2$). The CuO nano-foam was placed at the center of a quartz tube furnace that is equipped with optical radiate heater. The forming gas was flushed for 30 minutes at 40 sccm. The temperature was then increased to 300 °C using the optical heater at 30 °C/min. The heat treatment lasted for 30 minutes. After the heat source was turned off, the specimen cooled to room temperature while the reducing gas kept flowing. The overall shape of the final specimen is largely determined by the shape of electrospun template. A macroscopic fabric on the order of 70-80 mm in diameter reduces to a metal nano-foam about 20 mm in diameter, and the foam is on the order of 5-10 μ m thick using the process described here.

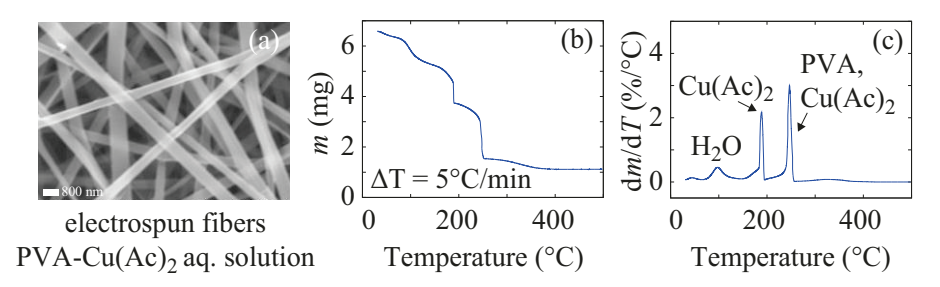


Figure 1 (a) Scanning electron microscopy image of the electrospun PVA-Cu(Ac)₂ fibers (scale bar = 800 nm) (b) Thermogravimetric analyses, and (c) dm/dT curve indicating characteristic peaks of the thermal decomposition of the metal acetate precursor and polymer template.

We used scanning electron microscopy (SEM) in a dual beam Quanta 650 Focused Ion Beam (FIB) to characterize the morphology of the nano-foams. Secondary electron images were used to determine the microscopic morphology of the nano-foam. Samples for transmission electron microscopy (TEM) were prepared using the FIB and an Omniprobe 200 (Oxford instruments Inc.) nanoscale manipulator to lift-out a Cu nano-foam section, which was subsequently attached to a Mo grid post. X-ray diffraction, with a Bruker D8 with Cu K- α ($\lambda = 1.5406$ Å) radiation, was used to identify the crystalline phases of the nano-foams over the range of $2\theta = 25^{\circ}$ to 55° at a scanning rate of 10 °/min. The TEM diffraction and imaging was carried out using a Tecnai T20 (FEI) equipped with a LaB6 thermionic source and a Gatan 4 megapixel camera. Selected area electron diffraction (SAED), bright field (BF) imaging and centered dark field (cDF) imaging were used to determine the polycrystalline structure of the Cu nanofoam from the cross-section. The mechanical property of the Cu nano-foam was measured by nano-indentation using a Hysitron Triboindenter 950 equipped with a flat cylindrical diamond tip with a diameter of 100 μm, [5, 6]. The flat-punch tip was used due to substantially variable microstructure of the nano-foam.

RESULT AND DISCUSSION

The morphology and thermogravimetric analysis (TGA) of the electrospun fiber fabric are shown in **Figure 1**. With increasing temperature, the total weight of the fiber sample decreases due to decomposition and evaporation of the Cu(Ac)₂ metal precursor and the pyrolysis of the polymer template. Thermogravimetric analyses for each component are reported elsewhere.[7-9] The characteristic decomposition peaks are significantly shifted to lower temperatures (by 80°C for electrospun PVA, and about 30-50°C for Cu(Ac)₂) than previously reported, suggesting the thermal decomposition of the Cu(Ac)₂-PVA mixture follows a different kinetic pathway than those of each individual component. The strong interaction between precursor-template has not been further investigated in this work.

After pyrolysis of the electrospun fiber at 500°C, a polycrystalline nanoscale foam structure made of nano-sized CuO grains is obtained, as shown in Figure 2. A notable difference is this structure no longer has the geometry of a non-woven fabric, but appears more three-dimensionally interconnected. A previous study by Lin et al. has shown the Cu(Ac)₂ almost completely transforms to CuO when heated above 500°C.[8] Because the nucleation occurs within the confined geometry set by the electrospun fiber, the short-range diffusion of the metal nuclei appears to lead to a conformative ligament

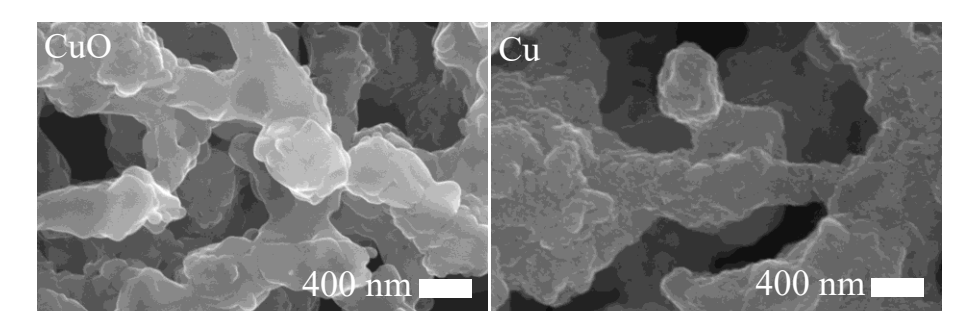


Figure 2 Scanning electron microscopy images of the CuO nano-foam after thermal process at 500°C, and Cu nano-foam after reducing process.

structure. The polycrystalline morphology may be a result of reducing the surface area, form equilibrium crystalline shape, and minimize the grain boundary interface energy of the nanoscale fine grain system. This CuO nano-foam is almost completely reduced to a Cu nano-foam under the reducing gas heat treatment. Since the size of the CuO ligament is on the order of 500 nm, penetration of reducing gas species appears to be efficient. After reduction the Cu nano-foam shows increased surface porosity.

The nodular morphology of the nano-foam is somewhat misleading, as the grain size seems to be similar to the size of each oxide nodule, however, a cross-section TEM analysis (**Figure 3**) shows the polycrystalline structure of the Cu nano-foam is finer than the oxide grain size. The cross-section shows two different types of pore structures that might be caused by different mechanisms. **Figure 3**(b) shows a typical pore that is also visible in SEM images, which originate from the initial separation between adjacent electrospun fibers. There are also substantially smaller scale pores, as shown in **Figure 3**(e), where the pore size is less than the metal grain size. This small pore is located at a triple point. We suggest this (and other) pores may be created during the reduction process with different oxygen and copper diffusivities. This fine pore structure is unexpected, and the presence of such fine pores reduce the density of each ligament, creating a notable deviation from the basic assumption of Gibson-Ashby model that will be discussed in the following section.

The elastic modulus and hardness of the Cu nano-foam was measured by flat punch nano-indentation (Figure 4). The load-depth curves, carried out in depth control, show significant point-to-point variations (Figure 4(a)). The variation in load-depth curves is due to spatial variations in density of the foam and the "flatness" of the initial surface contact; a protruding ligament can lead to an initially soft contact (the blue curve in Figure 4(a)), while other regions of the film show contact with more ligaments (the green and orange curves in **Figure 4**(a), respectively). Using the constant contact area of the 100 µm diameter tip and the unloading stiffness with the Sneddon's approximation as described by Oliver and Pharr, the elastic modulus and hardness of nano-foam were calculated and are shown in **Figure 4**(b,c). The perceived modulus varies between 0.1 and 6 MPa, while the hardness varies between 1 and 60 kPa orders of magnitude lower than one would expect for copper [10]. The residual impression of the flat-punch tip on the foam, **Figure 4**(d), shows both densification near the periphery of the indentation while the center of the indent site deformed into a sparse net geometry, showing that several strong ligaments connections remained after the indentation, suggesting lateral, tensile stretching of these ligaments, rather than the out-of-plane elastic recovery of a conventional solid, may dominate the unloading response of the load-depth

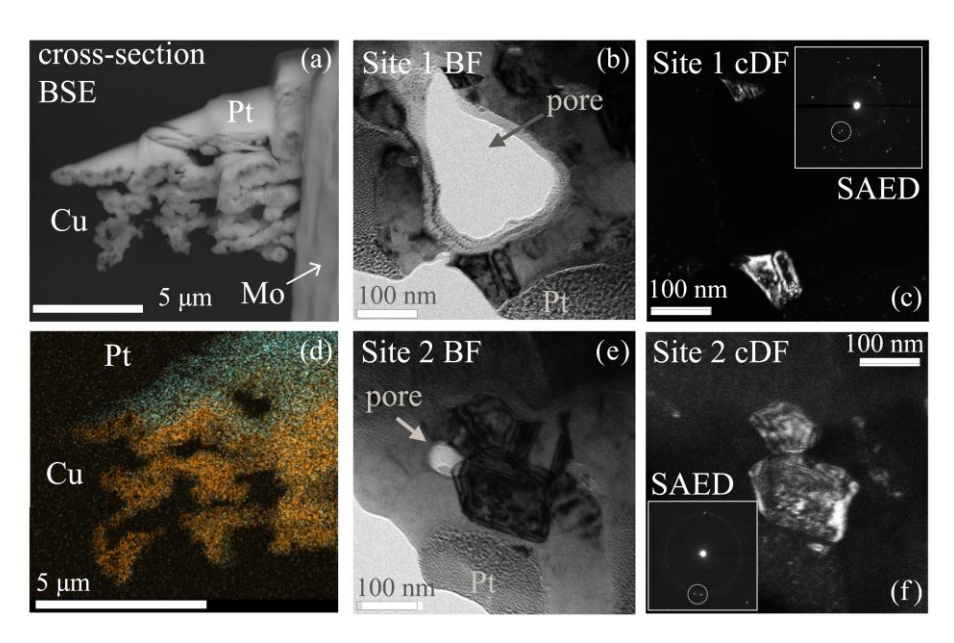


Figure 3 Electron microscopy images of the nano-foams. (a) Back scattered electron (BSE) images of the cross-section of Cu nano-foam mounted on Mo grid. (b) Bright field TEM image of Cu nano-foam featuring an interligament pore, (c) TEM centered dark field (cDF) image from the selected *g* reflections shown inset, (d) energy dispersive mapping of the sample, and (e,f) TEM BF image capturing a small pore between multiple grains, and the corresponding cDF image.

curve. However, other indentation measurements on porous metals (at higher relative densities of $\approx 30\%$) have observed the hardness or porous gold is on the order of 10-100 MPa, not kPa, and noted that the strength of a given ligament may be tied to the size of said ligament.[11]

The Gibson-Ashby model is widely used to predict the mechanical properties of porous materials based on the properties of the bulk material.[12, 13] Since the literature suggests the strength of a ligament may be dependent on size the elastic modulus may be more robust in relating the macroscopic density of a foam to the density of the solid material,

$$\rho_{\rm f} = \rho_{\rm s} \sqrt[n]{\frac{1}{c} \frac{E_{\rm f}}{E_{\rm s}}}$$

where $_{\rm f}$, $_{\rm s}$, $_{\rm f}$ and $_{\rm s}$ denote the density of the foam and bulk material, and the measured elastic modulus of the foam, and the bulk material respectively. For the case of cubic bending model in the original derivation of Gibson and Ashby,[12] the parameters in the equations can be approximated as C=1.0, and n=2, respectively. While this classic open cell cubic model has been widely accepted, however, the nano-foam presented in this work does not follow its general trend. The estimated macroscopic density of the foam in this study (mass divided by nominal external dimensions) was approximately 0.3 g/cm3 (a relative density of 3%). However using the measured modulus and hardness of the foam related to that of bulk copper (a modulus of \approx 100 GPa and a hardness of \approx 0.5 GPa), would lead to an estimated density shown in **Figure 4**(e), an order of magnitude lower than one would expect from the standard cubic open cell model calculation. Three possible explanations of this surprisingly low value are (1) that the foam contains significant non-connected ligaments and protrusions on ligaments (which cannot carry load) (2) the porosity within the ligaments is leading to substantially more compliant and

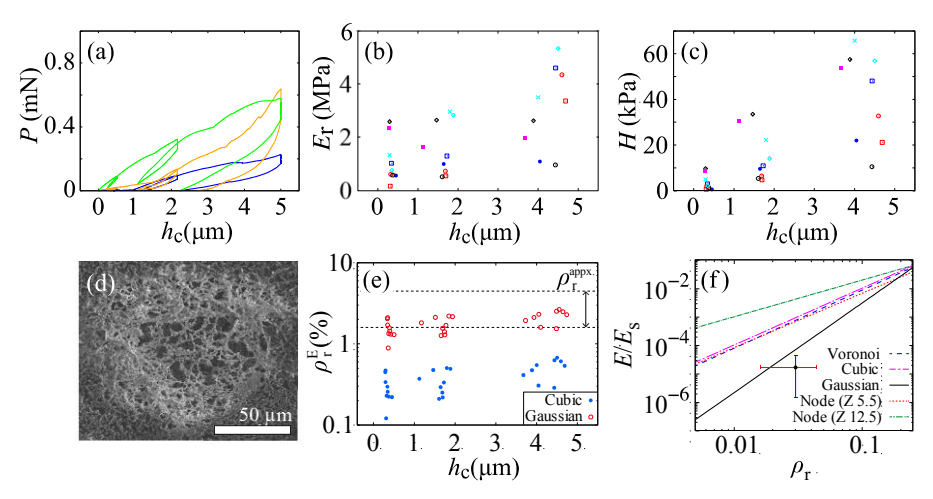


Figure 4 (a) Representative load-depth curves of Cu nano-foam, (b,c) reduced elastic modulus and hardness from load-depth curves using Oliver-Pharr method. (d) SEM image of a typical residual indentation impression, (e) relative density of the Cu nano-foam, where 100% corresponds to Cu bulk phase, as calculated by the cubic open cell model by Gibson-Ashby using the measured elastic modulus. The estimated density with range in order to give comparison. Notable deviation from the Gibson-Ashby model is due to porous ligand structure of the Cu nano-foam. (f) Relative scale modulus versus density plot according to several variations of the Gibson-Ashby model. The nano-indentation measurements are shown as a black circle with error bars. For the node network model, Z denotes the average coordination number of the network structure.

softer foams than if the ligaments were solid or (3) the 3% relative density means ligament stretching, not node bending, may be dominating the performance and different foam models are appropriate. When compared to different kinds of random cell models,[13] the nano-foam in the present work best matches to the least regular geometry among the five different models (Figure 4(f)). Still, the Gaussian random model does not address the multi-scale nature of the porous ligament.

In this work, we present a synthesis of a low-density ($\approx 3\%$) Cu foam with nanoscale ligaments, followed by thermal, microstructural and mechanical analyses. The fine grain, multi-scale porous structure of Cu nano-foam uniform over large area may be useful for many applications, but requires further exploration of our fundamental understanding of the domain of the strength and relative density. As an example, the mechanical property of the Cu nano-foam exhibits substantial deviation from the isomorphic cellular model, which may be caused by the hierarchical porosity present (the ligaments in the porous sample themselves are porous).

CONCLUSIONS

A Cu nano-foam was synthesized using electrospun polyvinyl alcohol nonwoven fibers as templates. As a result of thermal treatment, the polymeric fibers transform to CuO nano-foams which are then subsequently reduced to a Cu nano-foam. This resulted in a notable increase of surface roughness of the nano-foam. The finegrained porous structure of Cu was observed with TEM cross-section imaging. The strength and stiffness of the Cu nano-foam was measured by flat punch nano-indentation, and the low values of perceived modulus and hardness suggest that the fine porous and rough structure of ligament may be responsible for the observed decreases both the stiffness and hardness of the foam.

ACKNOWLEDGMENTS

This work was supported by the National Science Foundation under collaborative Grant Nos. CMMI 1634772 and CMMI 1634640

REFERENCES:

- 1. M. Hakamada and M. Mabuchi: Crit. Rev. Solid State Mater. Sci. 38, 262 (2013).
- I. McCue, E. Benn, B. Gaskey and J. Erlebacher: Annual Review of Materials Research 46, 263 (2016).
- 3. A. Greiner and J.H. Wendorff: Angew. Chem. Int. Ed. 46, 5670 (2007).
- H. Wu, L. Hu, M.W. Rowell, D. Kong, J.J. Cha, J.R. McDonough, J. Zhu, Y. Yang, M.D. McGehee and Y. Cui: Nano Lett. 10, 4242 (2010).
- D.F. Bahr and D.J. Morris: Nanoindentation: Localized probes of mechanical behavior of materials, in Springer Handbook of Experimental Solid Mechanics (Springer2008), p. 389.
- W.C. Oliver and G.M. Pharr: J. Mater. Res. 19, 3 (2004).
 M.D. Judd, B.A. Plunkett and M.I. Pope: J. Therm. Anal. Calorim. 6, 555 (1974).
- 8. Z. Lin, D. Han and S. Li: J. Therm. Anal. Calorim. 107, 471 (2012).
- 9. J. Liu, M.J. Chang and H.L. Du: Mater. Lett. 183, 318 (2016).
- 10. T.-H. Fang and W.-J. Chang: Microelectron. Eng. 65, 231 (2003).
- J. Biener, A.M. Hodge, J.R. Hayes, C.A. Volkert, L.A. Zepeda-Ruiz, A.V. Hamza and F.F. Abraham: Nano Lett. 6, 2379 (2006).
- M.F. Ashby and L.J. Gibson: Cellular solids: structure and properties, (Cambridge New York 1997), p. 186.
- 13. A.P. Roberts and E.J. Garboczi: J. Mech. Phys. Solids 50, 33 (2002).